Start Clim 2023

Glacial melt feedbacks to climate change: Losing a CH4-source but also a CO2-sink?

Bundesministerium
Klimaschutz, Umwelt,
Energie, Mobilität,
Innovation und Technologie

Bundesministerium
Bildung, Wissenschaft
und Forschung

klima+ energie fonds

LAND
OBERÖSTERREICH

ober österreich

umweltbundesamt

BOKU

Dalvai-Ragnoli Martin*, Gabriel Singer*

* Universität Innsbruck, Institut für Ökologie

Diese Publikation sollte folgendermaßen zitiert werden:

Dalvai-Ragnoli Martin; Gabriel Singer. (2024): Gletscherschmelze: Verlieren wir eine Methan-Quelle aber auch eine Kohlendioxid Senke? Endbericht von StartClim2023.E in StartClim2023: Biodiversität, Klimakippeffekte und sozioökonomische Klimaindikatoren, Auftraggeber: BMK, BMWFW, Klima- und Energiefonds, Land Oberösterreich.

Wien, im September 2024

StartClim2023.E

Teilprojekt von StartClim2023

Projektleitung von StartClim:

Universität für Bodenkultur, Department für Wasser – Atmosphäre – Umwelt

Institut für Meteorologie und Klimatologie, Gregor-Mendel-Straße 33, 1190 Wien

www.startclim.at

StartClim2023 wurde aus Mitteln des BMK, BMWFW, Klima- und Energiefonds und dem Land Oberösterreich gefördert.

Table of content

E-1 Kurzfassung 5
E-2 Abstract 6
E-2.1.1 Figures 7
E-2.1.2 Tables 9
E-3 Introduction 17
E-4 Methods 19
E-4.1 Study area and study design 19
E-4.2 Gas concentration and weathering capacity 19
E-4.3 Chemical parameters 20
E-4.4 Data analysis 21
E-5 Results 22
E-5.1 Dissolved CH4 concentration 22
E-5.1.1 Export of CH4 from the Glaciers 23
E-5.2 Dissolved CO2 concentration 24
E-6 Discussion 25
E-7 Conclusio 28
E-8 References 29

List of figures

Abb. E-1: Study design of sampling program including measured parameter at upstream sampling sites (S1) and downstream sampling sites (S2). 7

Abb. E-2: Conceptual diagram of processes involving greenhouse gas concentration in glacial meltwater streams. Arrows indicate direction of fluxes and chemical interactions. Processes increasing aquatic dissolved gas concentration are indicated in blue, processes contribution to decrease in dissolved gas concentration are indicated in red. 8

Abb. E-3: Overview map of the study area. Source: Open Street Map, Mosaic of Sentinel-2 satellite images acquired between June and July 2023 at 50-m resolution, coordinate system WGS 84/UTM. Country borders and initials are shown in yellow. Sampling sites are represented as red dots. 8

Abb. E-4: Example pictures of different glacier outlets and streambed structure: Pool-like outlet at the Furkeleferner (a), meandering stream through fine sediment at the Pasterze (b), steep fast flowing streams with coarse rocks Gaisbergferner (c) and on bedrock with bigger boulders at the Hornkees (d). 9

List of tables

Tab. E-1: Sampled Glaciers by Name, Country (C) and glacier ID. Glacier Area (in km2) and Glacier elevations (meter above sea level) from GLIMS. Mean and standard deviation of ice thickness (m) and glacier surface flow velocities for 2016 and 2018 in meters per year (Millan et al. 2022). 9

Tab. E-2: Coordinates (in UTM) and altitude (m.a.s.l.) of S1 sampling site for each glacier stream as well as average slope (%) and the distance(m) from S1 to S2, for streams with a second sampling site. 10

Tab. E-3: Measured chemical parameters 13

Tab. E-4: Overview of CH4 results: saturation (%) and dissolved concentration (µmol L-1) at S1. Change in dissolved concentration from S1 to S2 (µmol L-1), estimated discharge (Q; m3 s-1) and estimates for lateral CH4 transport (LT; gCH4 d-1). Some S1 sites had CH4 concentration below detection limit (BDL) of the GC. 14

Tab. E-5: Overview of CO2 results: saturation (%) and dissolved concentration (µmol L-1) at S1. Change in dissolved concentration from S1 to S2 (µmol L-1), weathering potential (µmol L-1) and saturation (%) at S2. 15

E-1 Kurzfassung

In hoch gelegenen Gebirgsregionen wie den Alpen sind die Auswirkungen der globalen Erwärmung durch die rasch schmelzenden Gletscher drastisch spürbar. Dieses Abschmelzen erschöpft nicht nur lebenswichtige Wasserreserven, sondern setzt auch erhebliche Mengen von gespeichertem Kohlenstoff frei, der zum Teil seit Jahrtausenden im Gletschereis eingeschlossen war. Die Mobilisierung gelöster Kohlenstoffverbindungen aus schmelzenden Gletschern stimuliert flussab biologische Prozesse und kann potenziell die Konzentration von gelöstem Kohlendioxid (CO2) erhöhen. Während dadurch eine CO2-Anreicherung in Gletscherbächen auftreten kann, könnte die effiziente Verwitterung von Karbonat-haltigen Sedimenten diesem Effekt entgegenwirken und atmosphärisches CO2 binden. Zusätzlich kann organischer Kohlenstoff, der unter Gletschern gespeichert ist, unter anoxischen Bedingungen durch mikrobielle Aktivität in Methan (CH4) umgewandelt werden, welches durch das Schmelzwasser aus dem Gletscher ausgetragen und an die Atmosphäre abgegeben werden kann. Obwohl diese Phänomene in arktischen Gletschern beobachtet wurden, fehlen Untersuchungen zu den Europäischen Alpen. In dieser Studie wollen wir das Treibhausgaspotenzial alpiner Gletscherbäche untersuchen. Wir haben Bäche von 26 Gletschern in den Ost- und Westalpen beprobt und umfassende Analysen von Gaskonzentrationen, Verwitterungskapazität und chemischen Parametern durchgeführt. Während die CH4-Werte für einige Standorte unterhalb der Nachweisgrenze lagen, waren alle anderen Gletscherbäche im Vergleich zur Atmosphäre übersättigt mit CH4. Die Gletschergröße war dabei einer der ausschlaggebenden Parameter. Die CH4 Konzentration in unseren Gletscherbächen lag in der gleichen Größenordnung wie die Konzentrationen von alpinen Quellbächen ohne glaziales Einzugsgebiet und von Schmelzwasser anderer kleiner Berggletscher, aber um Größenordnungen niedriger als die Konzentrationen, die im Schmelzwasser großer arktischer Gletscher gemessen wurden. Dennoch sind unsere alpinen, gletschergespeisten Bäche eine Quelle für CH4 an die Atmosphäre. Im Vergleich zu Emissionen aus arktischen Eismassen, die unsere alpinen Gletscher in Eisvolumen und Gletscherfläche bei weitem übertreffen, ist das Ausmaß der CH4 Emissionen gering. Im Vergleich zu CH4 war die CO2 Konzentration dynamischer, wobei einige Bäche als CO2-Senken und andere als CO2-Quellen fungierten. Zusätzlich scheinen - je nachdem ob es sich um eine CO2 Quelle oder Senke handelt - unterschiedliche Mechanismen die CO2-Dynamik zu beeinflussen. Unsere Ergebnisse deuten auch darauf hin, dass im Schmelzwasser einiger Standorte CO2 aktiv in Verwitterungsreaktionen verbraucht wurde. Diese Reaktionen mit frisch verwitterten Sedimenten waren demnach für eine Abnahme der CO2-Sättigung entlang des Bachlaufs mitverantwortlich. Für CO2 lässt sich somit nicht eine allgemein gültige Aussage treffen, vielmehr sind lokale chemische und geologische Faktoren dafür verantwortlich ob CO2 ausgegast oder aufgenommen wird. Basierend auf den in dieser Studie gesammelten Daten, insbesondere den beobachteten Konzentrationen, scheinen Gletscherbäche das Kohlenstoffbudget der Alpenregionen nicht wesentlich anders zu beeinflussen als andere Quellflüsse. Daher können alpine Gletscherbäche bei der Schätzung von Treibhausgasemissionen in größerem Maßstab, etwa für ein regionales Flussnetzwerk oder eine Provinz, ähnlich anderen Flüssen gleicher Größe behandelt werden.

E-2 Abstract

In high mountain regions like the Alps, the impacts of global warming are strongly felt and glaciers are melting rapidly. This melting not only depletes vital water reserves but also releases significant amounts of stored carbon, some of which has been trapped in glacier ice for millennia. The mobilization of dissolved organic carbon compounds from melting glaciers stimulates downstream biological processes, potentially increasing dissolved CO2 levels. While CO2 enrichment can thereby occur in glacier streams, efficient weathering of carbonate and silicate sediments downstream may counteract this effect, sequestering atmospheric CO2. Additionally, organic carbon stored beneath glaciers can be transformed into methane (CH4) by microbial activity under anoxic conditions. This strong greenhouse gas can then leave the glacier ecosystem as dissolved gas in the meltwater before being rapidly released into the atmosphere in the typically turbulent glacier-fed streams. Despite these phenomena being observed in Arctic glaciers, investigations regarding the European Alps are lacking. In this study, we aim to explore the greenhouse gas potential of alpine glacier streams by examining the presence of CH4 sources and CO2 sinks as well as the geochemical variables impacting these processes. We sampled streams from 26 glaciers in the Eastern and Western Alps (including glaciers in Italy, Austria and Switzerland) and conducted extensive analyses of gas concentrations, weathering capacity, and chemical parameters. Although for some sites CH4 levels were below detection limit, all other glacier streams were supersaturated in CH4 compared to the atmosphere. We investigated drivers for CH4 in our streams and found the size of glaciers to be amongst the most important predictors for CH4 concentration. Methane concentration in the streams was in the same order as concentrations reported from alpine headwater streams without glacierised catchments and from meltwater of other mountain glaciers. However, observed concentrations of CH4 were orders of magnitude lower than those reported in the meltwater of large arctic glaciers. Nevertheless, the investigated alpine glacier-fed streams were mostly a source of CH4 into the atmosphere. However, compared to emissions from arctic ice masses, which surpass our alpine glaciers in ice volume and glacier area, the magnitude of this CH4 source is weak. CO2 was more dynamic across the sampled streams, with some streams acting as a CO2 sink and others as a source of CO2 to the atmosphere. Furthermore, different mechanisms seem to be driving CO2 concentration in streams acting as a source compared to streams which are a CO2 sink. Similar to previous studies, our results indicate active consumption of CO2 in weathering reactions to be responsible for a decrease of CO2 saturation along the stream. Thus, for CO2 no general statement can be made as local chemical and geological conditions determine whether CO2 is released or taken up by the meltwater stream. Based on the data collected in this study, particularly the observed concentrations, glacier-fed rivers don't seem to impact the carbon budget of alpine regions disproportionately compared to other headwater streams. Therefore, when estimating GHG emissions on a larger scale, such as for a regional river network or Province, alpine glacier-fed rivers may be treated similarly to equal sized streams.

E-2.1.1 Figures

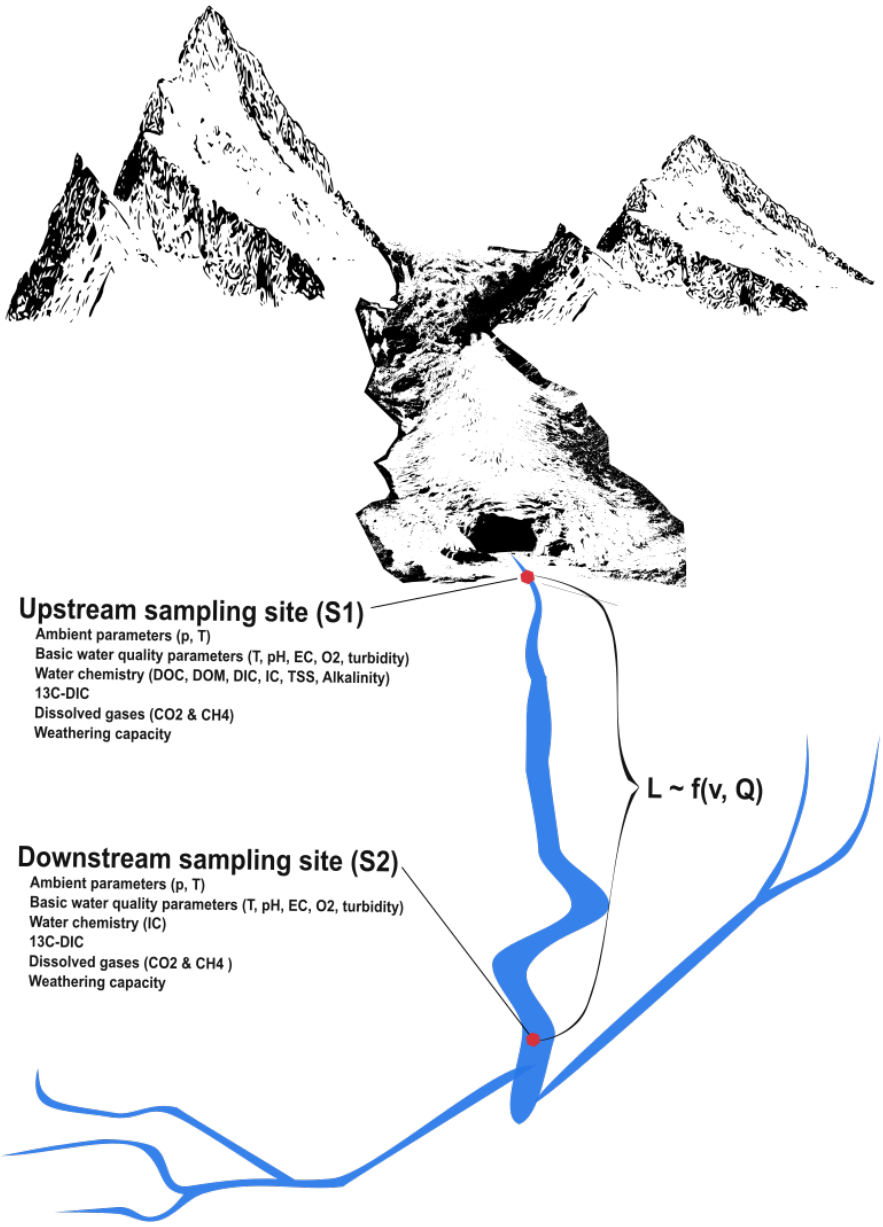

Abb. E-1: Study design of sampling program including measured parameters at upstream sampling sites (S1) and downstream sampling sites (S2).

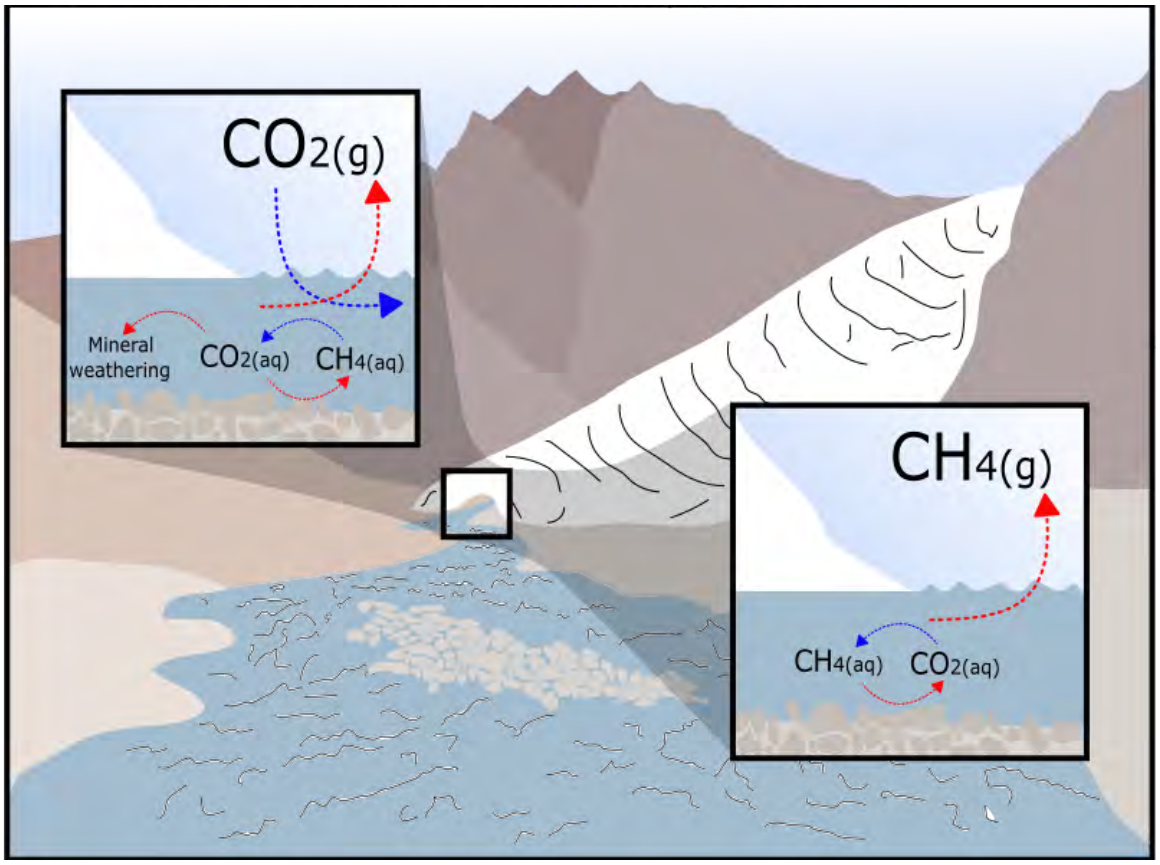

Abb. E-2: Conceptual diagram of processes involving greenhouse gases in glacial meltwater streams. Arrows indicate direction of fluxes and chemical interactions. Processes increasing aquatic dissolved gas concentration are indicated in blue, processes contributing to decrease in dissolved gas concentration are indicated in red.

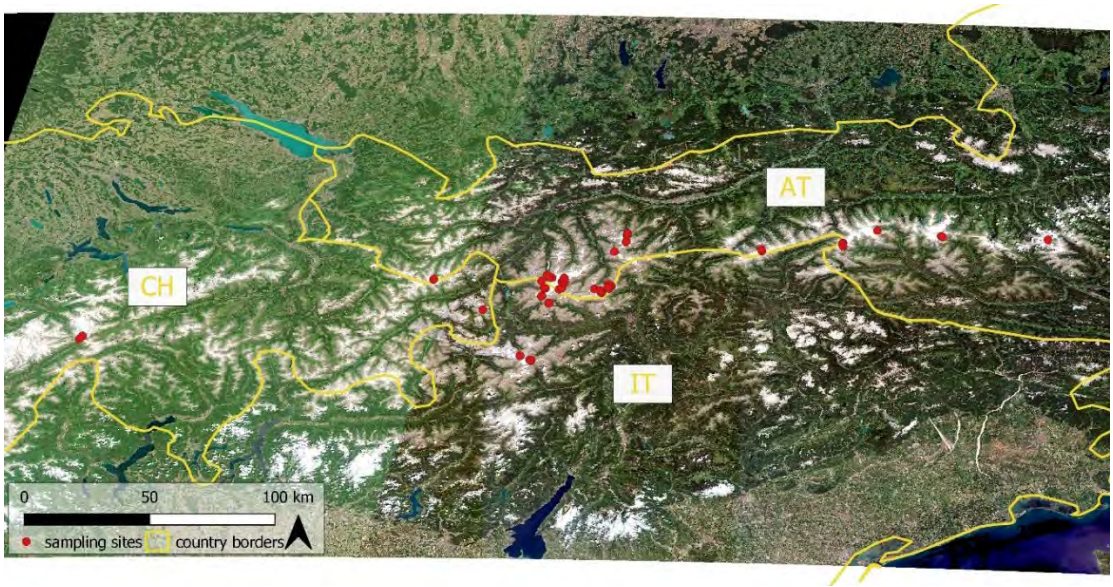

Abb. E-3: Overview map of the study area. Source: Open Street Map, Mosaic of Sentinel-2 satellite images acquired between June and July 2023 at 50-m resolution, coordinate system WGS 84/UTM. Country borders and initials are shown in yellow. Sampling sites are represented as red dots.

Abb. E-4: Example pictures of different glacier outlets and streambed structure: Pool-like outlet at the Furkeleferner (a), meandering stream through fine sediment at the Pasterze (b), steep fast flowing streams with coarse rocks Gaisbergferner (c) and on bedrock with bigger boulders at the Hornkees (d).

E-2.1.2 Tables

Tab. E-1: Sampled glaciers by name, country (C) and glacier ID. Glacier area (in km2) and glacier elevations (meter above sea level) from GLIMS. Mean and standard deviation of ice thickness (m) and glacier surface flow velocities for 2016 and 2018 in meters per year (Millan et al. 2022).

Glacier	C	Glacier ID	Area (km2)	Median elevation (m.a.s.l.)	Max elevation (m.a.s.l.)	Ice thickness (m)	Ice flow velocity (m yr-1)
Alpeiner	AUT	G011128E47046N	2.68	3051	3283	48.1 ± 38.7	9.8 ± 38.0
Furkele	IT	G010639E46452N	1.77	3175	3722	44.2 ± 25.2	7.2 ± 8.2
Gaisberg	AUT	G011066E46828N	0.85	3028	3338	23.6 ± 19.8	7.1 ± 34.8
Gepatsch	AUT	G010748E46850N	15.2	3093	3488	131.2 ± 82.7	12.2 ± 13.6

Gurgler	AUT	G010987E46794N	8.75	3000	3357	87.9 ± 64.0	5.5 ± 5.0
Guslar	AUT	G010822E46874N	1.07	3154	3441	30.8 ± 11.9	3.4 ± 2.2
Hintereis	AUT	G010752E46802N	7.7	3051	3674	54.5 ± 48.5	4.9 ± 4.3
Horn	AUT	G011817E47001N	2.71	2792	3214	32.4 ± 10.7	6.7 ± 5.5
Jamtal	AUT	G010144E46868N	3.06	2813	3107	31.1 ± 15.1	4.7 ± 4.3
Kleinelend	AUT	G013253E47062N	2.33	2870	3159	37.5 ± 31.5	11.7 ± 19.1
Langtaler	AUT	G011021E46784N	2.18	2900	3360	38.7 ± 28.2	3.3 ± 2.3
Langtauferer	IT	G010734E46818N	7.16	3193	3476	65.3 ± 61.1	6.8 ± 7.9
Lazaun	IT	G010742E46742N	0.07	3105	3289	13.9 ± 6.6	3.6 ± 1.7
Luesener	AUT	G011128E47086N	2.67	3009	3257	73.5 ± 64	27.5 ± 102.1
Matsch	IT	G010725E46789N	2.31	3236	3693	28.4 ± 12.4	4.4 ± 4.3
Pasterze	AUT	G012678E47096N	16.58	2984	3487	107.8 ± 87.8	25.7 ± 30.6
Rhone	CH	G008398E46623N	14.18	2982	3610	121.6 ± 100.9	20.9 ± 21.2
Rotmoos	AUT	G011042E46813N	2.39	2983	3394	24.24 ± 10.31	3.1 ± 2.7
Schlaten	AUT	G012386E47103N	7.77	3074	3576	70.03 ± 48.49	20.5 ± 23.6
Sesvenna	IT	G010410E46710N	0.36	2930	3050	57.67 ± 23.09	9.9 ± 3.7
Sulden	IT	G010571E46495N	4.03	2889	3723	21.23 ± 8.14	2.2 ± 1.4
Sulztal	AUT	G011080E47001N	2.85	2949	3243	40.65 ± 27.49	3.0 ± 2.5
Umbal	AUT	G012246E47058N	4.09	3006	3398	35.8 ± 18.17	7.6 ± 8.4
Vernagt	AUT	G010823E46875N	7.04	3142	3559	46.31 ± 30.78	4.2 ± 5.3
Weissee	AUT	G010713E46857N	2.33	2931	3475		
Zufall	IT	G010633E46456N	1.64	3199	3664	47.04 ± 27.63	6.7 ± 6.4

Tab. E-2: Coordinates (in UTM) and altitude (m.a.s.l.) of S1 sampling site for each glacier stream as well as average slope (%) and the distance (m) from S1 to S2 for streams with a second sampling site.

Glacier	UTM		Slope (%)	L to S2 (m)

Name	Z	E	N	Altitude (m.a.s.l.)		
Alpeiner	32T	662051	5213407	2715	21.33	450
Furkele	32T	627027	5146110	2864	26.5	200
Gaisberg	32T	657145	5188648	2558	21.68	143
Gepatsch	32T	634059	5192776	2282	9.9	909
Gurgler	32T	650537	5186812	2487		
Guslar	32T	637956	5190437	2948	16.5	1630
Hintereis	32T	636984	5186295	2482	7.46	1287
Horn	32T	714494	5209995	2328	28.8	1000
Jamtal	32T	588503	5190906	2530	26.77	310
Kleinelend	33T	368417	5213862	2416		
Langtaler	32T	653468	5184747	2533	11.44	306
Langtauferer	32T	631780	5186734	2656	11.74	690
Lazaun	32T	633021	5178513	2899	20.08	488
Lusener	32T	662289	5217399	2756	22.58	248
Matsch	32T	630512	5182511	2841	16.29	313
Pasterze	33T	327519	5216903	2327	7.53	823
Rhone	32T	453028	5158804	2320	21.76	2500
Rotmoos	32T	656270	5187088	2586	21.77	464
Schlaten	33T	303152	5220965	2353		
Sesvenna	32T	607772	5174206	2868	31.43	70
Sulden	32T	622708	5148619	2777	19.2	125
Sulztal	32T	657728	5207921	2761		
Umbal	33T	289736	5214419	2623	17.61	846
Vernagt	32T	638806	5192688	2978	34	300

Weissee	32T	630160	5190810	2858		

Tab. E-3: Measured chemical parameters

Glacier	TW	EC	O2		DOC	DN	DRSi	NH4	pH	Alk	DIC	HCO3	SO4	Cl	NO3	Ca	Mg	K	Na
	°C	µS cm-1	mg L-1	%	µg L-1	µg L-1	µg L-1	mg L-1		µeq L-1	µg L-1	g L-1	mg L-1	mg L-1	mg L-1	mg L-1	mg L-1	mg L-1	mg L-1
Alpeiner	2.3	26.8	10.2	102	509	184.6	342	0.025	7.71	92	1420	6.4	5.6	0.09	0.148	3.51	0.529	0.695	0.23
Furkele	0.1	272.7	10.1	97	734	177.8	695	0.034	7.42	120	2463	9.1	110.5	0.181	0.151	42.44	5.864	0.356	0.388
Gaisberg	0.9	164.4	10.6	102	206	115.4	215	0.032	8.59	538	5663	26.3	55.08	0.074	0.117	25.66	4.399	1.419	0.264
Gepatsch	0.4	25.4	11.4	103	484	72.9	206	0.029	7.81	70	735.2	3.6	8.7	0.107	0.048	3.36	0.716	0.49	0.17
Gurgler	1.5	85.6			1154	298.8	685	0.04	8.28	38	827.4	3.1	20.77	0.664	0.125	5.71	2.101	1.325	0.825
Guslar	0.2	36.1	10.4	101	611	56.1	450	0.028	5.17	22	289.7	0.2	12.02	0.134	0.018	2.3	1.031	0.956	0.186
Hintereis	0.6	149.1	11.2	103	1259	113.9	1731	0.08	6.44	25	459.9	1.1	60.83	0.472	0	16.53	4.87	2.358	0.956
Horn	4	6.1	10.3	102	276	105	107	0.03	6.62	38	728.8	2.2	0.57	0.103	0.082	1.18	0.063	0.243	0.122
Jamtal	3.2	25.8	10.5	84	1166	94.5	444	0.002	7.1	156	1725	8	4.61	0.084	0.042	4.11	0.423	0.224	0.33
Kleinelend	1.1	56.5	10.7	101	616	112.8	619	0.02	7.96	467	5688	28.2	2.98	0.095	0.111	9.81	0.345	1.415	0.365
Langtaler	1.4	39.8	9.6	92	462	80.7	294	0.029	7.92	121	1001	4.7	13.11	0.09	0.068	4.65	0.997	0.752	0.174
Langtauferer	0.6	368	10.2	96	587	127.9	2062	0.06	4.29	0	333.8	1.6	160.2	0.308	0.03	30.53	14.867	1.328	0.611
Lazaun	3.5	271.3	9.3	100	403	111	990	0.03	6.54	30	561.6	1.4	114.03	0.608	0.067	37.46	7.08	1.645	0.471
Luesener	0	11.1	10.6	101	401	136.9	201	0.007	7.78	93	1325	5.1	0.48	0.129	0.08	2.23	0.068	0.72	0.153
Matsch	2.3	106.2	9.9	99	888	125.2	1142	0.014	5.22	0	318.6	0.2	40.5	0.126	0.069	8.46	3.506	0.973	0.463
Pasterze	1.1	71.9	10.8	100	344	137.8	178	0.037	8.89	724	6919	34.6	5.65	0.095	0.113	12.75	0.776	0.992	0.105
Rhone	1.8	7.6	11.6	107	351	91.6	373	0.006	8.63	43	836.1	3.4	1.03	0.028	0.077	1.35	0.078	0.414	0.177
Rotmoos	3.4	109.9	9.9	101	304	127.5	267	0.009	8.22	658	8424	39.6	20.67	0.098	0.15	15.82	3.142	1.33	0.205
Schlaten	0.9	82.2	11.9	109	2544	161.9	260	0.031	8.29	436	5083	24.9	16.54	0.095	0.107	11.39	1.434	1.665	0.202
Sesvenna	0	10.7	10.5	99	335	48.7	103	0	7.82	58	1248	4.6	1.79	0.046	0.026	1.71	0.465	0.176	0.121
Sulden	-0.1	14.7	10.5	99	1421	197.6	29	0.115	7.96	78	1037	4.8	1.25	0.117	0.126	2.16	0.126	0.061	0.051
Sulztal	0.3	2	10.7	102	846	24.4	37	0	7.95	30	452.4	1.8	0.29	0.023	0	0.15	0.099	0.427	0.062
Umbal	1.8	67	10.4	101	503	188.8	291	0.035	7.93	299	3351	16.9	17.07	0.131	0.155	9.95	1.53	0.943	0.207
Vernagt	0.3	4.7	10.4	102	418	18.4	47	0.012	6.34	31	441.3	1.2	1.29	0.071	0	0.96	0.077	0.212	0.048
Weissee	0	4.2	10.7	101	267	22	30	0.008	7.05	34	588.1	2.2	0.38	0.021	0.01	0.8	0.126	0.125	0.039
Zufall	-0.1	100.6	10.2	98	459	118.2	197	0.034	8.27	515	5285	27.5	22.99	0.093	0.086	14.78	2.226	0.252	0.226

Tab. E-4: Overview of CH4 results: saturation (%) and dissolved concentration (µmol L-1) at S1. Change in dissolved concentration from S1 to S2 (µmol L-1), estimated discharge (Q; m3 s-1) and estimates for lateral CH4 transport (LT; gCH4 d-1). Some S1 sites had CH4 concentrations below detection limit (BDL).

Glacier	CH4 saturation (%)	CH4 (µmol L-1)	ΔCH4 (µmol L-1)	Q (m3 s-1)	LT CH4 (g d-1)
Alpeiner	530	0.02		2	49
Furkele	1493	0.05	-0.04	0.2	14
Gaisberg	542	0.02		2	52
Gepatsch		BDL		25	
Gurgler		BDL		6	
Guslar		BDL		1.5	
Hintereis	195	0.01		6	58
Horn		BDL		10	
Jamtal	1219	0.05	-0.03	5	349
Kleinelend	1147	0.04		0.5	28
Langtaler		BDL		4	
Langtauferer	312	0.01	0	1	15
Lazaun		BDL		0.3	
Luesener	1001	0.04	0	2.5	122
Matsch	157	0.01	0	2	14
Pasterze	1876	0.07	-0.04	8	751
Rhone	121	0	0	0.1	1
Rotmoos		BDL		0.5	
Schlaten	1242	0.05		3	188
Sesvenna	389	0.01	0	1	19
Sulden	165	0.01	0	0.1	1
Sulztal		BDL		1	

Umbal	1094	0.04	-0.01	2	103
Vernagt	285	0.01	0	4	54
Vernagt 2	155	0.01		4	30
Weissee		BDL		0.2	
Zufall	277	0.01	-0.01	0.05	1

Tab. E-5: Overview of CO2 results: saturation (%) and dissolved concentration (µmol L-1) at S1. Change in dissolved concentration from S1 to S2 (µmol L-1), weathering potential (µmol L-1) and saturation (%) at S2.

Glacier	CO2 saturation (%)	CO2 (µmol L-1)	ΔCO2 (µmol L-1)	Weathering potential (µmol L-1)	S2 CO2 saturation (%)
Alpeiner	139	28.13	-6.87	16.01	109
Furkele	282	60.84	-24.99	-5.53	172
Gaisberg	68	14.6	1.16	-5.58	75
Gepatsch	138	31.71	-1.66	15.87	137
Gurgler	127	27.07	14.62		
Guslar	148	31.51	-9.42	-13.93	113
Hintereis	150	33.46	-9.2	-2.12	114
Horn	131	26.15	-1.36	15.23	130
Jamtal	141	35.31	-6.63	-30.49	121
Kleinelend	177	38.2	22.95		
Langtaler	112	23.89	1.45	5.3	120
Langtauferer	136	29.81	5.67	-22.75	178
Lazaun	103	19.16	-4.35	3.2	109
Luesener	130	28.46	6.92	13.04	172
Matsch	124	25.3	-2.48	-13.79	119

Pasterze	121	27.07	2.6	7.02	135
Rhone	103	22.68	5.17	12.64	135
Rotmoos	110	21.43	-0.82	-28.08	114
Schlaten	154	34.63	-8.03		
Sesvenna	119	26.13	-0.5	9.64	119
Sulden	97	21.23	-2.12	11.17	94
Sulztal	108	23.61	9.88		
Umbal	173	36.28	-2.34	6.63	181
Vernagt	100	21.43	2.8	15.24	121
Vernagt 2	74	15.94			
Weissee	141	30.82	19.14		
Zufall	96	20.73	-5.45	-3.31	75

E-3 Introduction

In high mountain regions, the consequences of global warming are particularly noticeable because temperatures there are rising more rapidly than on the global average. As a result, in recent decades and especially in the Alpine region, glaciers are retreating at alarming rates. With this disappearance of glacier ice, we lose an important water reservoir and huge amounts of stored carbon (C) are released. Some of it has been stored in glacier ice for thousands of years (Hood et al., 2015). It is estimated that due to glacier melt, 9.86 Tg of dissolved C will be mobilized in the meltwater of alpine glaciers in the next 30 years (Hood et al., 2015). Furthermore, it has been shown that the released C compounds from melting glaciers in European glacier streams are chemically diverse and highly reactive, stimulating downstream heterotrophic biological processes (Singer et al., 2012). Dissolved C can thus stimulate primary production in aquatic habitats and lead to an increase in dissolved CO2. In glacier streams, this CO2 enrichment can be countered by the removal of CO2 through efficient weathering of carbonate sediments downstream (St Pierre et al., 2019). This process, leads to the sequestration of atmospheric CO2 and is known from Arctic glacier streams in Canada (St Pierre et al., 2019). However, its importance in alpine catchments has not been investigated. While in previous meltwater studies from alpine glaciers CO2 undersaturation in 65% of glacier streams was found (Singer et al., 2012), the possible CO2 storage capacity was not considered.

However, organic C is not only stored in glacier ice but also in the sediments beneath the ice masses. Recent studies show that ancient organic material in such glacial sediments is processed to CH4 under anoxic conditions by microbial activity (Burns et al., 2018; Jesper Riis Christiansen & Jørgensen, 2018; Lamarche-Gagnon et al., 2019). This CH4 is then dissolved in meltwater, transported to the glacier margin, and released into the atmosphere (Jesper R. Christiansen et al., 2021). This phenomenon has been observed so far at glaciers in Greenland, Iceland, and Canada, but investigations regarding European Alps are pending. If CH4 is also produced beneath alpine glaciers, it can be expected to quickly and efficiently outgas into the atmosphere due to the typically turbulent flow behaviour of glacier streams (Dalvai Ragnoli et al., 2023; Maurice et al., 2017; Ulseth et al., 2019).

The pronounced temporal dynamics in alpine glacier-fed streams, which are subject to particularly high diurnal and seasonal variations, influence flow regimes, discharge volume, and sediment load, which in turn affect production and degassing rates. Glacier streams are, therefore, particularly dynamic systems with a high gas exchange potential. The physical conditions in the high mountains combined with a continuous supply of organic C, dissolved CH4, and carbonate sediments from the glacier can influence climate change to an unknown extent. Since CO2 and CH4 are also the two most important greenhouse gases, it is important to understand the extent of these processes and key controlling factors to assess potential negative feedback processes between glacier melt and the associated release of greenhouse gases and further global warming.

In this project, we aim to address central questions regarding the greenhouse gas potential of alpine glacier streams. We want to test the hypothesis that glacier streams in the Alps can both (i) store atmospheric carbon through chemical binding, and (ii) release ancient organic carbon mobilized by glacier melt in the form of CH4. Through measurements along a regional gradient of different glaciers, we want to investigate whether and under what conditions these processes can also occur in alpine glaciers and identify the origin of the potentially respired carbon to CH4. Additionally, we aim to identify previously unknown sources and sinks in the regional greenhouse gas balance. The two central questions to be addressed in the study are:

Are alpine glacier streams CH4 sources and CO2 sinks? And which factors may control both processes? In detail:

1a) Are alpine glaciers environmentally similar to Arctic glaciers where organic material is processed into CH4 through microbial processes and carried out of the glacial ecosystem in meltwater?

1b) Are glacier streams characterized by CO2 undersaturation due to chemical weathering processes, resulting in an uptake of atmospheric CO2 from the meltwater?

2b) What geographical factors (geology, glacier size, altitude) act as crucial controls for the mentioned processes?

E-4 Methods

E-4.1 Study area and study design

We studied the streams of 26 glaciers in the Eastern and Western Alps and sampled each site once in the period of July to August 2023. At each glacier we sampled the meltwater stream as close as possible to the glacier outlet and, depending on accessibility and time, we took additional water samples further downstream.

The only constraint for the upstream sampling site (S1), to get as close to the glacier outlet, was due to accessibility and safety. The location of the downstream sampling site (S2) was aimed to be within the recommended separation length proposed for the open channel two-station method for ecosystem metabolism (Grace & Imberger, 2006). However, as we tried to measure the same water body downstream, to exclude a data bias due to temporal dynamics, we rather aimed to measure as promptly as possible rather than investing much time in hydraulic measurements needed for accurate definition of probe separation. Especially as glacier-fed streams typically experience a high variability of discharge even on sub-daily timescale, which in turn might affect composition of the meltwater (Lamarche-Gagnon et al., 2019). Additionally, the measurements of hydraulic parameters like discharge, depth and flow velocity are time-consuming and sometimes even impossible to get due to inaccessibility of the sites. Therefore, in the field, we calculated depth based on estimates of discharge, flow velocity and channel width to obtain the recommended distance between measurement points, also taking into account that for lower productive systems a wider probe separation is recommended (Grace & Imberger, 2006). Finally, the location of the downstream sampling point was also constrained due to accessibility to the stream.

We extracted the altitude and distance between sampling sites from Google Earth using the sampling site coordinates. Slope was computed as average slope in-between sites based on difference in altitude and distance. Glacier outlines, bedrock geology and mean elevation where obtained from the Global Land Ice Measurements from Space database (GLIMS & NSIDC, 2005), while glacier thickness and flow velocity was obtained from Millan et al. (2022).

E-4.2 Gas concentration and weathering capacity

Dissolved gas concentrations of CH_4 and CO_2 were measured using the head-space method and gas chromatography. Samples were taken in triplicate with a syringe by collecting 70 mL of water from 10 cm below the water surface and a gaseous headspace respectively. We used either N_2 (N_2>99.9%) brought into the field with gas bags or background air as gaseous headspace. Equilibration between the two phases was enhanced by intense shaking for approximately two minutes. We ensured equilibration at stream temperature by regularly submerging the equilibration syringe. The equilibrated gaseous headspace was then transferred into pre-evacuated gas vials and stored with over-pressure until analysis. For the gas analysis we used a gas chromatograph (GC, Shimadzu GC-2014, Japan) equipped with a thermal conductivity detector (TCD) for detection of CO_2 and a flame ionization detector (FID) for detection of CH_4 and, after conversion with a methanizer, for low CO_2 concentrations. From the thereby obtained headspace concentration, the equilibrium concentration of the water phase was computed using Henry's law of solubility at in-situ water temperature. The original water concentration was finally computed by summing the number of moles in the equilibrated phases and by accounting for background concentration if atmospheric air was used for equilibration.

CO_2 is, unlike CH_4, in a dynamic chemical equilibrium with other carbonate species in the water (Stumm & Morgan, 1981). Thereby, the exchange of CO_2 between water and headspace induces a change in the dissolved inorganic carbon (DIC) concentration, where CO_2 will be either produced from or converted to HCO_3^-. Therefore, we computed dissolved CO_2 concentration considering the chemical equilibration of the carbonate system in the equilibration vial. Thereby, pH was estimated

after equilibration from alkalinity by using the Rhs() function proposed by Koschorreck et al. (2020) and corrected for field pressure.

Gas saturation was computed as ratio between actual dissolved gas concentration and saturation concentration at complete equilibrium with the atmosphere. The latter was computed using Henry's law of solubility with an average of measured background gas concentration across all sites in combination with in-situ water temperature and atmospheric pressure.

To measure the capacity of the system for chemical weathering we collected unfiltered water samples in 20 mL gas vials, which contained 4 mg of NaN3 to kill biological activity. Immediately upon return to the laboratory a 10 mL headspace of N2 (N2>99.9%) was injected into the vials by extracting an equal volume of sample. The vials were stored in order for weathering reactions to proceed to equilibrium without CO2 exchange with the atmosphere. Subsequently, CO2 concentration in the headspace was measured using gas chromatography. To compute the dissolved concentration of the equilibrated samples, we calibrated the GC with two standard solutions. Solutions were prepared by bubbling a gas standard with known CO2 concentration through a water column and by computing the dissolved concentration using Henry´s law.

E-4.3 Chemical parameters

In the field, ambient temperature and pressure were measured using a barometer. In-situ water temperature, conductivity, dissolved oxygen, and pH were measured using a WTW handheld probe (Xylem Analytics, Germany) at 10 cm depth at a well-mixed location.

Water samples for DOM were collected using plastic syringes and filtered through pre-rinsed 0.2 µm membrane filters (Sartorius). DOM was characterized by spectroscopic analysis. Fluorescence intensities were measured at excitation wavelengths ranging from 250 to 450 nm (5 nm increments) and emission wavelengths from 350 to 550 nm (4 nm increments) using a Fluoromax-4 Spectrofluorometer (Horiba). Absorbance was measured with a Spectrophotometer (Hitachi).

Immediately upon return to the laboratory, unfiltered water samples were filtered through pre-weighed glass fibre filters (Whatman GF/F), cooled and stored in the dark until analysis. Dissolved ions (Cl-, NO3--N, SO4-2, Na+, K+, Mg2+, Ca2+) were analysed with an Ion Chromatograph (Dionex ICS, Thermo Sceintific, USA), dissolved reactive silicon was measured with a flow analyser (scalar, Netherlands), and DOC, DIC and total dissolved nitrogen concentrations were analysed with a TOC Analyzer (Shimadzu TOC – TNM, Japan). Alkalinity was measured by titration.

Total suspended solids (TSS) were measured gravimetrically from the pre-weighed filters and the organic fraction was obtained by the mass loss after combustion at 350 °C. Turbidity was measured from a bulk water sample using a portable turbidity meter (Turb 430 IR/T, WTW, Xylem Analytics, Germany).

To measure δ13C-DIC we filtered bulk water samples through pre-rinsed 0.2 µm membrane filters (Sartorius) and by avoiding turbulences of the filtrate. Samples were measured using a gas chromatograph interfaced to an isotope ratio mass spectrometer (IRMS) (Thermo Scientific). Briefly, 2-5 mL of sample were injected into a He-filled exetainer, containing 0.5-1.5 mL 85% H3PO4 and intensively shaken for approximately 10 minutes. The evolved CO2 was purged from the exetainer through a double-needle sampler into a He-carrier stream. The CO2 was passed to the IRM through a Poroplot Q GC column. Isotopic composition is reported in reference to Vienna Pee Dee Belemnite (VPDB).

E-4.4 Data analysis

All data analysis was performed using the software R (version 4.3.2) and the package ggplot2 (version 3.5.1) was used for visualization. Linear regressions were done using the lm() function. Maps of sampling sites were created using the program QGIS (version 3.28.2).

To further explore which drivers influence the investigated processes of CH4 emission and or CO2 sequestration in our glacier streams we built random forest models using our data as training data for the model. Models were built using the randomForest R package (version 4.7-1.1) and we used 500 independent decision trees and 5 randomly selected predictors at each split to evaluate the importance of our different predictor parameters on the response variables. To reduce dimensionality in our dataset we performed a principal component analysis (PCA) for DOM data and for chemical parameters. The Kaiser-Guttman Criterion was used for determination of number of used principal components in the models. PCA was done using the R package FactoMineR (version 2.9) and factoextra (version 1.0.7) for visualization.

E-5 Results

We sampled all 26 glacier streams once in June and July 2023. Differences in hiking time to get to individual glaciers made it impossible to align the sampling time. However, all glaciers were sampled during daylight hours in between 8 am and 6 pm. Observed discharge at the time of sampling varied in between streams from 0.1 to 25 m3 s-1.

The glacier outlets differed widely in their hydraulic properties: from pool-like to meander-like sections and fast flowing turbulent sections. Glacier streams featured a wide range of different streambed structures from bedrock to coarse boulders and fine sediments as well as different characteristics from steep sections, small waterfalls to meandering streams and pool riffle sections. Streambed slope in between sampling sites varied widely from a minimum of 7.5% to a maximum of 34 % (mean 20 ± 7.4%). However only two streams would be classified as moderately steep (<8%), while 33% would be classified as steep (<18%) and 62% as very steep (>18%).

Water temperature of the sampled streams was low, which comes as no surprise as it is meltwater from glacial ice. Water temperature also influences gas solubility, as cold water is able to hold more dissolved gases. Mean water temperature at S1 sites was 1.2 ± 1.2 °C. Concentration of dissolved oxygen was above or close to saturation given atmospheric concentration (mean of O2 saturation 101. 4%) for all sites, showing that our turbulent glacier streams were well-mixed with the atmosphere. Thereby we could on one hand preclude any significant possible anoxic subglacial contribution but on the other hand subglacial CH4 could already have been lost due to oxidation or emission processes upstream of our sampling site.

Ionic composition of glacial meltwater typically varies on a diurnal and seasonal scale (Hubbard & Glasser, 2005; Pain et al., 2021). Therefore, the measured chemical parameters are to be seen as a snapshot during the time of sampling. The most abundant cation and anion in all glacial streams were Ca2+ and HCO3- respectively. High HCO3-concentration can be explained by pH (mean pH of all S1 sites was 7.34 ± 1.15) as in between a pH of 6 to 9 the majority of DIC exists as HCO3- (Skidmore et al., 2004). The order of most abundant ions afterwards was SO42- > Cl- > NO3- for the anions and Mg+ > K+> Na+ for cations. While Cl-, Na+ and parts of SO42- are atmospherically derived solutes, HCO3-, SO42-, Ca2+, Mg+, K+ and Na + are solutes originating from chemical weathering of geologic material (Tranter et al., 1996). The same order in ion dominance was previously reported in glacial streams from Canada (Sapper et al., 2023), which highlights similarities in the chemical composition of the meltwater. Electrical conductivity and DOC in our glacier streams varied from 2 to 368 µS cm-1 (mean 82 ± 95 µS cm-1) and from 206 to 2544 µg L-1 (mean 675 ± 505 µg L-1), respectively.

Mean values of the atmospheric background CO2 and CH4 concentration (391 and 1.88 ppm, respectively), across all sites, were very close to the global mean for June and July 2023 (Ian Tiseo, 2023). Our values, also highly correlated with the measurements of a high mountain weather station in Austria during the days of sampling (Sonnblick.net, 2024). Therefore, we used mean background concentration across all sites in combination with in-situ water temperature and atmospheric pressure to compute dissolved equilibrium concentration for each site.

E-5.1 Dissolved CH4 concentration

Methane concentration was below detection limit at 32% of S1 sampling sites (minimal measured gas concentration by the GC was 0.8 ppm). However, all sites where CH4 was detected where supersaturated compared to the atmosphere. Mean supersaturation was 657 ± 543% with a median of 407% and highest supersaturation was at 1876%. However, the extreme supersaturation values are mostly attributed to the low pressure at the sampling sites resulting in low equilibrium concentration with the atmosphere (mean of 0.003 µmol L-1) rather than to high dissolved CH4 concentrations. In addition, low water temperature (1.2°C on average) does enable the water body to

hold more dissolved gases. Mean dissolved CH4 concentration at S1 sites was at 0.02 ± 0.02 µmol L-1, with a median concentration of 0.01 µmol L-1 and a maximum of 0.07 µmol L-1.

From upstream to downstream sampling sites the water temperature in each stream as well as atmospheric pressure increased (on average by 2°C and 9 hPa, respectively). While the increase of water temperature results in a decrease of gas solubility, the increase in pressure increases the ability of a water body to hold dissolved gas. Therefore, with respect to gas solubility, both changes tend to balance each other out. From upstream to downstream sampling sites, we did detect a loss of dissolved CH4 for 75% of our investigated glacier streams. Mean loss of dissolved CH4 (ΔCH4) was 0.01 ± 0.02 µmol L-1 (with a maximum loss of 0.04 µmol L-1). We found no influence of distance nor slope in between sampling sites with ΔCH4 (R2 in a linear regression of 0.06 and 0.03, respectively). At S2 CH4 supersaturation decreased to 410 ± 340 % and 93% of S2 were still supersaturated when compared to atmospheric equilibrium. We explain the high saturation levels at S2 in accordance to explanation for high S1 saturation values as result of low hypothetical equilibrium concentration with the atmosphere, rather than on high dissolved CH4 concentrations. Mean dissolved CH4 concentration at S2 sites was at 0.01 ± 0.01 µmol L-1, with a median concentration of 0.01 µmol L-1 and a maximum of 0.04 µmol L-1. The loss of CH4 from S1 to S2 can again be attributed to two processes, which are CH4 oxidation in and diffusive emission from the turbulent stream.

The result of a random forest model investigating main predictors for CH4 indicates aquatic CO2 to be by far the most important driver for dissolved CH4 concentration. Thereafter, equally influential on the dissolved CH4 concentration are the glacier area, the principal component representing alkalinity, NO3 and DIC as well as a PC representing dissolved organic material.

E-5.1.1 Export of CH4 from the Glaciers

Accurately calculating gas flux between the water phase and the atmosphere was beyond the scope of this study. Previous studies used discharge-weighted mean CH4 concentration from a longer measurement period and estimates of the gas transfer velocity to obtain a first estimate of diffusive CH4 emission from glacial streams (Lamarche-Gagnon et al., 2019). To compute the gas transfer velocity, these authors used stream velocity measurements from tracer injections in combination with established hydraulic relationships (Raymond et al., 2012). However, for steep mountain streams (>10%) these empirical models highly underestimate gas transfer (Ulseth et al., 2019) and our current understanding of mechanisms controlling gas transfer in steep streams is limited (Long et al., 2015). Gas exchange is known to increase with streambed roughness (Ulseth et al., 2019) and small waterfall sections - as found in our streams - are known to increase turbulence and local evasion rates (Leibowitz et al., 2017; Natchimuthu et al., 2017). Additionally, gas transfer, and thus evasion potential, increases with increasing discharge (Peter et al., 2014; Raymond et al., 2012; Zappa et al., 2007). Therefore, temporal variability in gas transfer is higher than spatial variability (Maurice et al., 2017).

As measurements of hydraulic parameters, needed to estimate the gas transfer velocity, were not possible in our systems, and the glacier streams where highly variable in their discharge, even on a sub-daily scale, we refrain from computing emission fluxes. Instead, we estimate the amount of laterally exported CH4 from the glacial ecosystems at the moment of sampling. Lateral CH4 transport was computed by multiplication of dissolved CH4 concentration with estimated discharge for each S1 site. This snapshot estimation was upscaled to daily export by simple multiplication with time.

Accumulated lateral CH4 export from all the sampled glaciers was estimated to be 1850 gCH4 per day. Mean export was 100 ± 180 g d-1 with a median of 30 g d-1. Highest export was observed for the Pasterze, the largest sampled glacier, due to combination of the highest recorded CH4 concentration with a respectable discharge.

E-5.2 Dissolved CO2 concentration

CO2 concentration was computed by both a simple sum of mole approach and by considering the chemical equilibration of the carbonate system in the equilibration vial. Comparison of the two methods for samples taken at S1 sites resulted in a mean error of 0.6 ± 1 %. Koschorreck et al. (2020) report the magnitude of the error to be strongly correlated to pH, as high pH is accompanied by low pCO2 for a given alkalinity. Thus, the error is typically below 10% at pH < 8 and can be further reduced by lowering equilibration temperature (Koschorreck et al., 2020). Given only 26% of our sites exhibited a pH above 8 and the low water temperature used to equilibrate (maximum recorded temperature of 4°C and mean 1.1 ± 1.2 °C) the low error does not come as a surprise. Therefore, as deviation error between methods was low and as at S2 sampling sites alkalinity measurements are lacking, we used the simpler sum of mole approach to compute the dissolved CO2 concentration for our samples.

Compared to atmospheric equilibrium 17% of S1 sampling sites where under-saturated in CO2. Mean CO2 concentration across all S1 sites was 27.5 ± 8.9 µmol L-1 (with a median of 26.2 µmol L-1), which is slightly higher than average atmospheric equilibrium concentration (21.5 µmol L-1). As a result, mean CO2 saturation was 128± 40% and minimal measured CO2 saturation was 70%. However, bottle essay experiments would suggest that weathering reactions were still actively occurring in the streams, as for 63% of the sites CO2 concentration was lower after incubation than in-stream measured concentration. This indicates, that weathering reactions did not yet reach equilibrium with the atmosphere at the time of sampling. In fact, at 67% of S2 sites CO2 concentration was lower compared to upstream sampling sites. According to a random forest model using chemical parameters as predictors the most important driver for the weathering potential were O2 saturation, concentrations of Mg+, SO42-, NH4 and Ca+, water temperature, electrical conductivity, dissolved inorganic carbon concentration as well as alkalinity of the water. Strong influence of ion concentration supports the presence of carbonate and silicate weathering reactions consuming aquatic CO2.

According to a random forest model the main predictor for CO2 concentration across all streams was CH4 concentration, followed by a set of principal components of chemical parameters and DOC concentration. Those PCs include NH4 concentration, water temperature, O2 saturation, turbidity and total dissolved solids as well as SO42- and Mg+ concentration as well as dissolved reactive silicon and electrical conductivity.

Loss of dissolved CO2 in the stream can happen due to atmospheric evasion for super-saturated water bodies or due to consumption of CO2 in weathering reactions. From our dataset we cannot identify the mechanisms behind the change in aquatic CO2 from S1 to S2. However, results from bottle essays suggest consumption of CO2 in weathering reactions at least for some of the systems. Changes in aquatic CO2 concentration were small for sites with decreasing CO2 concentration as well as for sites with an increase in aquatic CO2. Mean loss of CO2 was 5.6 ± 6.3 µmol L-1, while mean increase was 3.7 ± 2.2 µmol L-1. However, when drivers of CO2 concentration for streams which loose CO2 and streams with increasing CO2 are investigated separately, different importance in predictors emerge. For streams which lose CO2 similar predictors, except DOC concentration, as across all streams prevail. In contrast, in streams with increasing CO2 concentration the most important predictors are a principal component consisting mostly of total suspended solids, turbidity and dissolved nitrogen, as well as a set of principal components of dissolved organic material properties and DOC concentration. The change in predictors would suggest that different mechanisms are responsible for the respective changes in CO2 concentration in the streams.

E-6 Discussion

Although, all S1 sites, where CH4 concentration was above the detection limit, where supersaturated compared to the atmosphere, methane concentration in our glacier streams was in the same order as concentrations reported from alpine headwater streams without glacierised catchment (Crawford et al., 2014; Flury & Ulseth, 2019; Kuhn et al., 2017; Qu et al., 2017) and other low order streams (Dalvai Ragnoli et al., 2023; Stanley et al., 2016; Wallin et al., 2018). Du et al. (2022) report supersaturation of CH4 in the meltwater from a high mountain glacier in China, which features similar glacier size and CH4 concentration levels as glaciers in this study. Konya et al. (2024) investigated CH4 concentration in the runoff water of four smaller comparable mountain glaciers in Alaska. While only one of the four glaciers featured elevated CH4 levels, CH4 in the other three was two orders of magnitude lower and within the range found in this study. Although the four glaciers investigated by Konya et al. (2024) do not differ in bedrock geology and size, the variability in dissolved CH4 levels across glaciers highlights the importance of different CH4 production rates in different subglacial sediments (Stibal et al., 2012).

However, CH4 levels from our Alpine glaciers are orders of magnitude lower than concentrations reported in the glacial meltwater from Iceland (Burns et al., 2018), Greenland (Jesper R. Christiansen et al., 2021; Dieser et al., 2014; Lamarche-Gagnon et al., 2019) or Canada (Sapper et al., 2023). Ionic composition in the meltwater from our alpine streams is comparable to compositions reported from three glacial streams in Canada (Sapper et al., 2023). However, concentration of dissolved organic carbon and CH4 in those streams (DOC 7500 ± 2600 mg L-1 and CH4 0.523 ± 0.38 µmol L-1, respectively) are orders of magnitude above concentrations found in our alpine streams. Especially the higher DOC concentration indicates the higher availability of organic carbon for metabolic pathways. Compared to those three arctic glaciers our glaciers are also at least an order of magnitude smaller in size.

We have two not necessarily exclusive explanations for low CH4 values found in our glacier streams. First the low CH4 concentration can be a result from CH4 emission and /or oxidation upstream of our sampling site, which would mean we did not capture true CH4 concentration exported from the glaciers. We sampled the meltwater as close as safely possible to the glacier outlet. However, the meltwater was already well oxygenated, which indicates possibility of oxidation of CH4 as well as previous gas exchange with the atmosphere upstream of our sampling site. Although contribution of oxidation in turbulent glacier systems can be low (1% of exported CH4, Lamarche-Gagnon et al., 2019) diffusive emission is not transport-limited in turbulent reaches (Dalvai Ragnoli et al., 2023; Mønster et al., 2020). Thus, the possibility that we missed high CH4 concentration cannot be discharged, especially as recent findings show that in very steep (>18%) and moderately steep (4-8%) streams, as we were dealing with, gas transfer occurs within the first 100 up to 400 meters (Maurice et al., 2017).

Our second explanation ascribes low CH4 concentration in meltwater from alpine glaciers to glacier size and ice thickness. Whilst large glaciers and ice sheets have abundant subglacial sediments due to their sizable ice masses and additionally provide favourable temperature and pressure conditions for methanogens (Wadham et al., 2008, 2012), relatively small alpine glaciers could lack those conditions. The smaller ice surface could in turn also lead to better subglacial oxygen availability additionally favouring aerobic respiration of organic material. This hypothesis is supported by our model results, where glacier size is amongst the most important predictors for CH4 and by previous studies reporting no microbial CH4 production in subglacial sediments from an Alpine glacier in Switzerland (Zhu et al., 2018). Additionally, the glacier with the largest ice surface in our sample (Pasterze, 16.58 km2) featured highest measured CH4 concentration. However, low DOC concentrations in our streams compared to meltwater from arctic glaciers can also indicate generally lower carbon availability for microbial decomposition.

The two main mechanisms leading to a loss of aquatic CH4 are oxidation and evasion into the atmosphere. As contribution of oxidation in glacial streams is low compared to evasion (Lamarche-

Gagnon et al., 2019) and due to the high gas transfer potential in our streams, one can assume that all the CH4 exported from the subglacial domain is emitted to the atmosphere. However, we still want to point out that we provide conservatives estimates for lateral CH4 export. Recorded concentrations could have been influenced by oxidation and diffusive emission upstream of the measurement site, which would lead to an underestimation of lateral methane export. Additionally, our gas concentrations are derived from measurements taken at a single time and do not represent an average of a longer measurement period. Thus, variability in dissolved gas concentration even on a sub-daily scale cannot be represented by our samples. As a consequence, also our estimates for lateral export represent a snapshot in time and likely do not capture potential pulses of CH4 outbursts from the glaciers. This is especially important, as both pulses and dynamics of CH4 concentration on a seasonal as well as diurnal timescale, have been previously observed for glacier streams (Jesper R. Christiansen et al., 2021; Du et al., 2022; Lamarche-Gagnon et al., 2019). On top of that, also the discharge of alpine glacier streams is highly variable with daytime, weather and season. Therefore, more accurate emission estimates for alpine glacier streams should integrate both concentration and discharge dynamics.

As a direct result of the significantly lower CH4 concentration levels also our estimate for accumulated CH4 export from the sampled alpine glaciers (1.85 kgCH4 d-1) is lower than reported values from arctic glaciers. Burns et al. (2018) who sampled a glacier in Iceland, where geothermal activities favour CH4 production, report 41 tonnes of CH4 exported per day from a single glacier. Cumulative CH4 export from the Leverett Glacier in Greenland was estimated at 1.87 tonnes over the whole melting period, which rival emission from major world rivers (Lamarche-Gagnon et al., 2019). Compared, to those sizable ice masses, CH4 from smaller alpine glaciers seem neglectable.

Bottle essay experiments suggest weathering reactions to not yet have reached the equilibrium with the atmosphere at the time of sampling. Thereby CO2 consumption would still actively occur in the streams and thus, the sites acting as CO2 sinks would be underestimated. In fact, only 17% of sites were undersaturated in CO2 compared to the atmosphere but at 67% of S2 sites we observed a lower CO2 concentration compared to respective upstream sampling site. Degrees of saturation are consistent with results for a global glacier synthesis, which finds dissolved CO2 concentration to be at or near atmospheric equilibrium for all glaciers (Graly et al., 2017). However, 63% of S1 sites were supersaturated in CO2, which would imply, that glacial meltwater streams act as both sink and source of CO2 to the atmosphere. Differences in CO2 dynamics imply a variability in carbon processes in these glacial meltwater streams. Such spatial heterogeneity has been previously observed for glaciers on the Greenland Ice Sheet with differing underlying lithologies and has been attributed to differences in the relative magnitudes of microbial and geochemical processes interacting with CO2 (Pain et al., 2021).

Different drivers emerging from models for glacier streams losing and gaining CO2 in-between sampling points suggest different mechanisms responsible for the respective processes. Variability in CO2 concentration and thus direction of CO2 flux was previously reported from mountain glaciers in China (Du et al., 2022) and Alaska (Konya et al., 2024). Canadian mountain glaciers feature little temporal variability in CO2 but were consistently a sink of CO2 (Sapper et al., 2023). A high heterogeneity in CO2 dynamics is also reported for glacial meltwater at the Greenland Ice shield, where CO2 is consumed by mineral weathering throughout the melt season but difference in the magnitude of CO2 availability results in meltwater being either a source or a sink (Pain et al., 2021). Sub-glacially, CO2 can originate from organic matter remineralization (Graly et al., 2017; Pain et al., 2021) and, in accordance our model results, CO2 and DOC concentrations were reported to correlate in the glacial meltwater (Du et al., 2022).

The results of our random forest models predict CO2 and CH4 to be also the main predictor for the respective other gas, which suggest a strong linkage between these two gases. (Inverse) correlation in CH4 and CO2 was previously reported in one out of four investigated Alaskan mountain glaciers (Konya et al., 2024). While CO2 can result from CH4 oxidation in the presence of O2 or other electron

acceptors (Bastviken, 2009), CH4 resulting from CO2 reduction was previously observed in well oxygenated headwater streams (Flury & Ulseth, 2019). The presence of anoxic micro zones can also lead to simultaneous production of CH4 and CO2 in streambed sediment (Baker et al., 1999). In glacial meltwater a mixture of CH4 originating from acetate fermentation and from CO2-reduction was reported from the Leverett glacier (Lamarche-Gagnon et al., 2019). Thus, transformation pathways from one to the other greenhouse gas cannot be excluded in glacial meltwater streams.

Given the spatial variability in dissolved greenhouse gases observed in this study, constraining the impacts of the major biogeochemical, hydrologic and geologic controls on emission flux will be crucial for estimates on likely heterogeneous atmospheric GHG fluxes from glacial meltwater and to predict future impacts of ice loss on the greenhouse gas budget of changing alpine landscapes suffering loss of glaciers. However, more accurate estimates can only be achieved with improved data availability. Consequently, from our current knowledge standpoint, the logical next step is to conduct a more detailed investigation on fewer systems focusing on higher temporal resolution. These studies should prioritize examining the temporal variabilities of GHG dynamics on both diurnal and seasonal scales, aspects that were not addressed in the current study.

Glaciers selected for further investigation should be chosen based on now available data in the here presented study, while ideally also including variable geological backgrounds. The focus should primarily be on larger Alpine glaciers, where the signal - especially for the stronger greenhouse gas CH4 - is expected to be more pronounced, even though this may skew the data towards larger glaciers. In contrast to the here presented study, future research should also aim to capture the beginning of the melting season, as meltwater from glacier-fed streams typically has the highest dissolved GHG concentrations at that time, with typically decreasing patterns as the season progresses (Jesper R. Christiansen et al., 2021). However, especially early in the melting season accessing glacier streams in high alpine terrain can be particularly challenging, as thin layers of snow and ice still prevent access. Furthermore, single-point samples can lead to inaccurate emission estimates as diurnal variability is linked to glacial hydrology and runoff patterns. Thus, a higher temporal sampling resolution is required also on a diurnal scale. Capturing temporal patterns would thus require grab samples across various time scales, which presents a significant logistical challenge and is labour-intensive. A solution may be continuous in-situ measurements of dissolved GHGs by automatic loggers, but this has so far remained technologically challenging especially for CH4. Further, long-term installation of automatic measuring equipment in hydrologically variable high-alpine environments is demanding, often leading to burial of equipment under sediment or complete loss.

E-7 Conclusio

Spatial upscaling exercises have identified rivers and other freshwater ecosystems as significant emitters of CO2 and CH4 into the atmosphere on a global scale, yet headwater streams are often underrepresented in the literature, and their contributions remain poorly constrained. Based on the data collected in this study, in particular the observed concentrations, we can assume that glacier-fed rivers do not play a disproportionate role in the carbon budget of alpine regions compared to headwater streams in general, albeit slightly different mechanisms may be at work. We note that this judgement puts aside that temporal dynamics remain unclear. Unlike Arctic glacier meltwater, which acts as a significant CO2 sink due to weathering reactions on a watershed-scale (St Pierre et al., 2019), the here presented results show a high variability in CO2 dynamics from Alpine glacier streams. Moreover, these systems likely do not differ significantly in their CH4 emissions from non-glacierized alpine headwater streams (Flury & Ulseth, 2019). They are unlikely to rival the large emissions from Arctic glacier streams or large tropical rivers (Lamarche-Gagnon et al., 2019) or even from other freshwater systems like reservoirs, which, even in high alpine regions, are a significant source of CH4 emissions to the atmosphere (Delsontro et al., 2010). Thus, in eventual extrapolations to estimate GHG emissions for a larger spatial scale, e.g. a regional river network, Austria or a province thereof, it appears permissible to treat glacier-fed rivers similarly to other rivers or streams of similar size. Upscaling GHG emissions is usually done by multiplication of concentration gradients with independent estimates of gas exchange velocity and stream area. Here, the latter two variables convey much variability to the resulting emission estimate, suggesting that additional effort to empirically constrain concentrations in area-wise little important glacier-fed streams should be balanced by additional efforts on improving estimation of gas exchange velocity and stream area. Should future emission estimates be based on categorized concentration estimates, i.e. systems like glacier-fed streams be recognized on their own, then a closer look into temporal dynamics is recommended.

E-8 References

Baker, M. A., Dahm, C. N., & Valett, H. M. (1999). Acetate retention and metabolism in the hyporheic zone of a mountain stream. Limnology and Oceanography, 44(6), 1530–1539. https://doi.org/10.4319/lo.1999.44.6.1530

Bastviken, D. (2009). Methane. In Encyclopedia of Inland Waters (pp. 783–805). Elsevier Inc. https://doi.org/10.1016/B978-012370626-3.00117-4

Burns, R., Wynn, P. M., Barker, P., McNamara, N., Oakley, S., Ostle, N., Stott, A. W., Tuffen, H., Zhou, Z., Tweed, F. S., Chesler, A., & Stuart, M. (2018). Direct isotopic evidence of biogenic methane production and efflux from beneath a temperate glacier. Scientific Reports, 8(1), 1–8. https://doi.org/10.1038/s41598-018-35253-2

Christiansen, Jesper R., Röckmann, T., Popa, M. E., Sapart, C. J., & Jørgensen, C. J. (2021). Carbon Emissions From the Edge of the Greenland Ice Sheet Reveal Subglacial Processes of Methane and Carbon Dioxide Turnover. Journal of Geophysical Research: Biogeosciences, 126(11), e2021JG006308. https://doi.org/10.1029/2021JG006308

Christiansen, Jesper Riis, & Jørgensen, C. J. (2018). First observation of direct methane emission to the atmosphere from the subglacial domain of the Greenland Ice Sheet. Scientific Reports, 8(1), 1–6. https://doi.org/10.1038/s41598-018-35054-7

Crawford, J. T., Lottig, N. R., Stanley, E. H., Walker, J. F., Hanson, P. C., Finlay, J. C., & Striegl, R. G. (2014). CO2 and CH4 emissions from streams in a lake-rich landscape: Patterns, controls, and regional significance. Global Biogeochemical Cycles, 28(3), 197–210. https://doi.org/10.1002/2013GB004661

Dalvai Ragnoli, M., Schwingshackl, T., Kattus, S., Lissy, J., Wenninger, E., & Singer, G. (2023). Differential controls on CO2 and CH4 emissions from the free-flowing Neretva River, Bosnia and Herzegovina. Natura Sloveniae, 25(3), 213–237. https://doi.org/10.14720/ns.25.3.213-237

Delsontro, T., Mcginnis, D. F., Sobek, S., Ostrovsky, I., & Wehrli, B. (2010). Extreme methane emissions from a swiss hydropower Reservoir: Contribution from bubbling sediments. Environmental Science and Technology, 44(7), 2419–2425. https://doi.org/10.1021/es9031369

Dieser, M., Broemsen, E. L. J. E., Cameron, K. A., King, G. M., Achberger, A., Choquette, K., Hagedorn, B., Sletten, R., Junge, K., & Christner, B. C. (2014). Molecular and biogeochemical evidence for methane cycling beneath the western margin of the Greenland Ice Sheet. ISME Journal, 8(11), 2305–2316. https://doi.org/10.1038/ismej.2014.59

Du, Z. H., Wang, L., Wei, Z. Q., Liu, J. F., Lin, P. L., Lin, J. H., Li, Y. Z., Jin, Z. Z., Chen, J. Z., Wang, X. X., Qin, X., & Xiao, C. De. (2022). CH4 and CO2 observations from a melting high mountain glacier, Laohugou Glacier No. 12. Advances in Climate Change Research, 13(1), 146–155. https://doi.org/10.1016/j.accre.2021.11.007

Flury, S., & Ulseth, A. J. (2019). Exploring the Sources of Unexpected High Methane Concentrations and Fluxes From Alpine Headwater Streams. Geophysical Research Letters, 46(12), 6614–6625. https://doi.org/10.1029/2019GL082428

GLIMS, & NSIDC. (2005). Global Land Ice Measurements from Space glacier database(2005, updated 2018). Compiled and made available by the international GLIMS community and the National Snow and Ice Data Center, Boulder CO, U.S.A. https://doi.org/10.7265/N5V98602

Grace, M., & Imberger, S. (2006). Stream Metabolism : Performing & Interpreting Measurements. New South Wales Department of Environmental Conservation Stream Metabolism Workshop May, 31(September), 204. http://www.sci.monash.edu.au/wsc/docs/tech-manual-v3.pdf

Graly, J. A., Drever, J. I., & Humphrey, N. F. (2017). Calculating the balance between atmospheric CO 2 drawdown and organic carbon oxidation in subglacial hydrochemical systems. Global Biogeochemical Cycles, 31(4), 709–727. https://doi.org/10.1002/2016GB005425

Hood, E., Battin, T. J., Fellman, J., O'neel, S., & Spencer, R. G. M. (2015). Storage and release of organic carbon from glaciers and ice sheets. Nature Geoscience, 8(2), 91–96. https://doi.org/10.1038/ngeo2331

Hubbard, B., & Glasser, N. F. (2005). Field techniques in glaciology and glacial geomorphology. John Wiley & Sons.

Ian Tiseo. (2023). Globally-averaged, monthly mean atmospheric methane (CH4) abundance from 1990 to 2023. https://www.statista.com/statistics/1314344/atmospheric-concentration-of-ch4-historic-monthly/

Konya, K., Sueyoshi, T., Iwahana, G., Morishita, T., Uetake, J., & Wakita, M. (2024). CH4 emissions from runoff water of Alaskan mountain glaciers. Scientific Reports, 14(1), 1–9. https://doi.org/10.1038/s41598-024-56608-y

Koschorreck, M., Prairie, Y., Kim, J., & Marcé, R. (2020). Technical note: CO2 is not like CH4 – limits of and corrections to the headspace method to analyse pCO2 in water. Biogeosciences Discussions, 1–12. https://doi.org/10.5194/bg-2020-307

Kuhn, C., Bettigole, C., Glick, H. B., Seegmiller, L., Oliver, C. D., & Raymond, P. (2017). Patterns in stream greenhouse gas dynamics from mountains to plains in northcentral Wyoming. Journal of Geophysical Research: Biogeosciences, 122(9), 2173–2190. https://doi.org/10.1002/2017JG003906

Lamarche-Gagnon, G., Wadham, J. L., Sherwood Lollar, B., Arndt, S., Fietzek, P., Beaton, A. D., Tedstone, A. J., Telling, J., Bagshaw, E. A., Hawkings, J. R., Kohler, T. J., Zarsky, J. D., Mowlem, M. C., Anesio, A. M., & Stibal, M. (2019). Greenland melt drives continuous export of methane from the ice-sheet bed. Nature, 565(7737), 73–77. https://doi.org/10.1038/s41586-018-0800-0

Maurice, L., Rawlins, B. G., Farr, G., Bell, R., & Gooddy, D. C. (2017). The Influence of Flow and Bed Slope on Gas Transfer in Steep Streams and Their Implications for Evasion of CO 2. Journal of Geophysical Research: Biogeosciences, 122(11), 2862–2875. https://doi.org/10.1002/2017JG004045

Millan, R., Mouginot, J., Rabatel, A., & Morlighem, M. (2022). Ice velocity and thickness of the world's glaciers. Nature Geoscience, 15(2), 124–129. https://doi.org/10.1038/s41561-021-00885-z

Mønster, J., Fuglsang, K., & Riis Christiansen, J. (2020). Continuous methane concentration measurements at the Greenland ice sheet-atmosphere interface using a low-cost, low-power metal oxide sensor system. Atmospheric Measurement Techniques, 13(6), 3319–3328. https://doi.org/10.5194/amt-13-3319-2020

Pain, A. J., Martin, J. B., Martin, E. E., Rennermalm, Å. K., & Rahman, S. (2021). Heterogeneous CO2and CH4content of glacial meltwater from the Greenland Ice Sheet and implications for subglacial carbon processes. Cryosphere, 15(3), 1627–1644. https://doi.org/10.5194/tc-15-1627-2021

Peter, H., Singer, G. A., Preiler, C., Chifflard, P., Steniczka, G., & Battin, T. J. (2014). Scales and drivers of temporal pCO2 dynamics in an Alpine stream. Journal of Geophysical Research: Biogeosciences, 119(6), 1078–1091. https://doi.org/10.1002/2013JG002552

Qu, B., Aho, K. S., Li, C., Kang, S., Sillanpää, M., Yan, F., & Raymond, P. A. (2017). Greenhouse gases emissions in rivers of the Tibetan Plateau. Scientific Reports, 7(1), 1–8. https://doi.org/10.1038/s41598-017-16552-6

Raymond, P. A., Zappa, C. J., Butman, D., Bott, T. L., Potter, J., Mulholland, P., Laursen, A. E., McDowell, W. H., & Newbold, D. (2012). Scaling the gas transfer velocity and hydraulic geometry in streams and small rivers. Limnology and Oceanography: Fluids and Environments, 2(1), 41–53. https://doi.org/10.1215/21573689-1597669

Sapper, S. E., Jørgensen, C. J., Schroll, M., Keppler, F., & Christiansen, J. R. (2023). Methane emissions from subglacial meltwater of three alpine glaciers in Yukon, Canada. Arctic, Antarctic, and Alpine Research, 55(1). https://doi.org/10.1080/15230430.2023.2284456

Singer, G. A., Fasching, C., Wilhelm, L., Niggemann, J., Steier, P., Dittmar, T., & Battin, T. J. (2012). Biogeochemically diverse organic matter in Alpine glaciers and its downstream fate. Nature Geoscience, 5(10), 710–714. https://doi.org/10.1038/ngeo1581

Skidmore, M., Sharp, M., & Tranter, M. (2004). Kinetic isotopic fractionation during carbonate dissolution in laboratory experiments: Implications for detection of microbial CO2 signatures using δ13C-DIC. Geochimica et Cosmochimica Acta, 68(21), 4309–4317. https://doi.org/10.1016/j.gca.2003.09.024

Sonnblick.net. (2024). https://www.sonnblick.net/de/daten/zeitreihen/messung-co2/

St Pierre, K. A., St Louis, V. L., Schiff, S. L., Lehnherr, I., Dainard, P. G., Gardner, A. S., Aukes, P. J. K., & Sharp, M. J. (2019). Proglacial freshwaters are significant and previously unrecognized sinks of atmospheric CO2. Proceedings of the National Academy of Sciences of the United States of America, 116(36), 17690–17695. https://doi.org/10.1073/pnas.1904241116

Stanley, E. H., Casson, N. J., Christel, S. T., Crawford, J. T., Loken, L. C., & Oliver, S. K. (2016). The ecology of methane in streams and rivers: patterns, controls, and global significance. Ecological Monographs, 86(2), 146–171. https://doi.org/10.1890/15-1027

Stibal, M., Wadham, J. L., Lis, G. P., Telling, J., Pancost, R. D., Dubnick, A., Sharp, M. J., Lawson, E. C., Butler, C. E. H., Hasan, F., Tranter, M., & Anesio, A. M. (2012). Methanogenic potential of Arctic and Antarctic subglacial environments with contrasting organic carbon sources. Global Change Biology, 18(11), 3332–3345. https://doi.org/10.1111/j.1365-2486.2012.02763.x

Stumm, W., & Morgan, J. J. (1981). Aquatic Chemistry: An Introduction Emphasizing Chemical Equilibria in Natural Waters (Environmental Science and Technology: A Wiley-Interscience Series of Texts and Monographs) 2nd Edition. https://www.scirp.org/(S(351jmbntvnsjt1aadkposzje))/reference/ReferencesPapers.aspx?ReferenceID=2052039

Tranter, M., Brown, G. H., Hodson, A. J., & Gurnell, A. M. (1996). Hydrochemistry as an indicator of subglacial drainage system structure: A comparison of alpine and sub-polar environments. Hydrological Processes, 10(4), 541–556. https://doi.org/10.1002/(sici)1099-1085(199604)10:4<541::aid-hyp391>3.0.co;2-9

Ulseth, A. J., Hall, R. O., Boix Canadell, M., Madinger, H. L., Niayifar, A., & Battin, T. J. (2019). Distinct air–water gas exchange regimes in low- and high-energy streams. Nature Geoscience, 12(4), 259–263. https://doi.org/10.1038/s41561-019-0324-8

Wadham, J. L., Arndt, S., Tulaczyk, S., Stibal, M., Tranter, M., Telling, J., Lis, G. P., Lawson, E., Ridgwell, A., Dubnick, A., Sharp, M. J., Anesio, A. M., & Butler, C. E. H. (2012). Potential methane reservoirs beneath Antarctica. Nature, 488(7413), 633–637. https://doi.org/10.1038/nature11374

Wadham, J. L., Tranter, M., Tulaczyk, S., & Sharp, M. (2008). Subglacial methanogenesis: A potential climatic amplifier? Global Biogeochemical Cycles, 22(2). https://doi.org/10.1029/2007GB002951

Wallin, M. B., Campeau, A., Audet, J., Bastviken, D., Bishop, K., Kokic, J., Laudon, H., Lundin, E., Löfgren, S., Natchimuthu, S., Sobek, S., Teutschbein, C., Weyhenmeyer, G. A., & Grabs, T. (2018). Carbon dioxide and methane emissions of Swedish low-order streams—a national estimate and lessons learnt from more than a decade of observations. Limnology and Oceanography Letters, 3(3), 156–167. https://doi.org/10.1002/lol2.10061

Zappa, C. J., McGillis, W. R., Raymond, P. A., Edson, J. B., Hintsa, E. J., Zemmelink, H. J., Dacey, J. W. H., & Ho, D. T. (2007). Environmental turbulent mixing controls on air-water gas exchange in marine and

aquatic systems. Geophysical Research Letters, 34(10), L10601. https://doi.org/10.1029/2006GL028790

Zhu, B., Henneberger, R., Weissert, H., Zeyer, J., & Schroth, M. H. (2018). Occurrence and Origin of Methane Entrapped in Sediments and Rocks of a Calcareous, Alpine Glacial Catchment. Journal of Geophysical Research: Biogeosciences, 123(12), 3633–3648. https://doi.org/10.1029/2018JG004651